

Impact of Earthquake Action on the Design and Sizing of Jointed Masonry Structures in South Kivu, DRC

Edmond Dawak Fezeu^{1,2*}, Marcelline Blanche Manjia^{1,2},
Chérif Bishweka Biryondeke^{1,3}, Patient Kubuya Binwa³,
Élodie Rufine Zang^{1,2}, Chrispin Pettang^{1,2}

¹Laboratory of Engineering Civil and Mechanics, Doctoral Research Unit for Engineering and Applications, University of Yaoundé I, Yaoundé, Cameroon

²Department of Civil Engineering, National Advanced School of Engineering, University of Yaoundé I, Yaoundé, Cameroon

³Department of Civil Engineering, Faculty of Applied Sciences and Technologies, Free University of Great Lakes Countries, Goma, DRC

Email: *edmonddawakfezeu@gmail.com

How to cite this paper: Dawak Fezeu, E., Manjia, M.B., Bishweka Biryondeke, C., Kubuya Binwa, P., Zang, É.R. and Pettang, C. (2024) Impact of Seismic Action on the Design and Sizing of Jointed Masonry Structures in South Kivu, DRC. *Open Journal of Civil Engineering*, 14, 127-153.
<https://doi.org/10.4236/ojce.2024.141007>

Received: October 21, 2023

Accepted: March 26, 2024

Published: March 29, 2024

Copyright © 2024 by author(s) and Scientific Research Publishing Inc. This work is licensed under the Creative Commons Attribution International License (CC BY 4.0).

<http://creativecommons.org/licenses/by/4.0/>



Open Access

Abstract

This article deals with the investigation of the effects of seismic impacts on the design and dimensioning of structures in South Kivu. The starting point is the observation of an ambivalence that can be observed in the province, namely the non-consideration of seismic action in the study of structures by both professionals and researchers. The main objective of the study is to show the importance of dynamic analysis of structures in South Kivu. It adopts a meta-analytical approach referring to previous researches on South Kivu and proposes an efficient and optimal method. To arrive at the results, we use Eurocode 7 and 8. In addition, we conducted static analysis using the Coulomb method and dynamic analysis using the Mononobe-Okabe method and compared the results. At Nyabibwe, the results showed that we have a deviation of 24.47% for slip stability, 12.038% for overturning stability and 9.677% for stability against punching through a weight wall.

Keywords

Jointed Masonry Weight-Bearing Structures, Seismic Action, Eurocode 7 and 8, Static and Dynamic Analysis

1. Introduction

The earth's crust is the foundation for every building. In this sense, it deserves

careful attention in the analysis of its behavior towards internal and external seismic effects, since these strongly influence the interaction between any structure and the earth's envelope. Among the seismic actions that have the most destructive and irreversible effects on the balance of load-bearing structures (walls), seismic loads are among the most catastrophic. They always require constant attention from researchers, especially those in civil engineering, as the occurrence of this natural phenomenon has often cast doubt on the various theories and usual calculations of the stability of supporting structures (walls) [1] [2] [3].

In addition, a composite masonry weight wall is designed to retain a solid mass of land (embankment, soil) and hold it at a steeper slope than it might assume without the work. Because of this functionality, grouted masonry gravity walls are an important part of the built infrastructure. They are used for a variety of purposes, including securing traffic routes (roads, railroads, bridges, etc.), landslides, landslides and for quay walls and underground parking garage walls [4].

Studies on the stability of the seismic effects of jointless masonry walls have begun in recent decades and continue to develop, especially in regions where the risk of a seismic event is relatively high, such as the DR Congo, the United States or Japan. Seismic loading studies are generally based on analytical methods that consist of including a seismic acceleration or an inertial force in the equilibrium equations of the soil-structure system. In addition, physical and numerical models are sometimes used to clarify the response of these structures, even if it is far from being well understood [5] [6] [7] [8] [9]. Authors (Parishad Rahbari *et al.* (2017) [10]; I. E. Kilic *et al.* (2021) [11]; Sam M. B. Helwany (2001) [12]; Tufan Cakir (2013) [13]; George papazafeiropoulos *et al.* (2009) [14]; Adnan Falih Ali Christelle Létoffé (2013) [15]; Gupta H. *et al.* (2022) [16]) have investigated the behaviour of masonry walls under seismic action and recommend that the horizontal seismic inertia force be considered in the studies. This force can lead to significant displacements and deformations or even destruction of the structure. The design and dimensioning of an interactive, scalable, collaborative structure that is more accessible and adaptable to all phases of construction is of particular interest and importance to researchers and professionals [17].

South Kivu is one of the provinces of the Democratic Republic of Congo where there is a high seismic risk. It should also be noted that there were at least 534 earthquakes of magnitude 5 in eastern DRC between 1973 and 2008, most of them in South Kivu [18] [19] [20]. However, the literature shows that the studies in South Kivu are not thorough. In a province with seismic risk, a design and dimensioning standard is indeed more than necessary because it includes zoning of the seismic impact on the area, appropriate design and calculation approaches, but also optimal execution methods. Unfortunately, there is still no specific standard dealing with this issue in South Kivu, so that each planner has to consider the measures and calculation methods of his choice, in some cases even

neglecting or arbitrarily taking them into account. The immediate consequence of this situation therefore lies partly in the difficulty of ensuring the stability of gravity walls made of joint masonry during a pre- or post-seismic period.

We believe that in order to solve the above problem, researchers must be interested in the seismic stresses of the jointed masonry gravity walls in South Kivu. Static design without considering the dynamic aspect would leave the structure to ruin in the event of a seismic phase. Similarly, theories may lead to superimposing the effects of static or gravity forces and inertia forces due to seismic loads in the design of composite masonry gravity walls. In order to ensure the stability of precast masonry gravity walls in this region, designers must also incorporate seismic effects into the analysis of the behavior of these structures [21] [22] [23] [24] [25].

The overall objective of this thesis is to contribute to the current state of knowledge on the study of the stability of jointless masonry walls subjected to seismic loads in order to analyze their effects in South Kivu. These are:

- Determine the seismic risk in South Kivu;
- Evaluate the masonry gravity wall by performing a static and a dynamic analysis;
- Compare the two analyses;
- Evaluate the effects of seismic actions in the study of grouted masonry weight walls.

Eurocode 7 and 8 are used to obtain the results. The Coulomb and Mononobe-Okabe (M-O) methods are used to determine the total shear (total active pressure) in the static and dynamic calculations respectively. The analytical approach is presented. The numerical approach (software mainly based on finite element theory) is not discussed. The study is applied to Nyabibwe in the province of South Kivu in the DR Congo, which is a seismic risk area.

This work will help reduce the risk of seismic damage to support structures in South Kivu.

2. Methods

2.1. Characteristics of the Study Environment

2.1.1. Presentation of the Study Area: Nyabibwe

A trapezoidal gravity wall is currently under construction in South Kivu, in the town of Nyabibwe, in the Kalehe region, at the intersection of latitude 2°5'47" south and longitude 28°54'12" east, around 100 km north of the city of Bukavu and 100 km south-west of the city of Goma. As shown in **Figure 1**, the center of Nyabibwe lies to the west of Lake Kivu (a lake located to the east of the Kalehe region) and borders the Ndindi River (Bujuki sub-village) to the south-west, the Kumbi sub-village (Mweha sub-village, which is also part of the main village of Kabulu) to the east, the Nyamishongariver to the north-east and the village of Mianzi to the west.

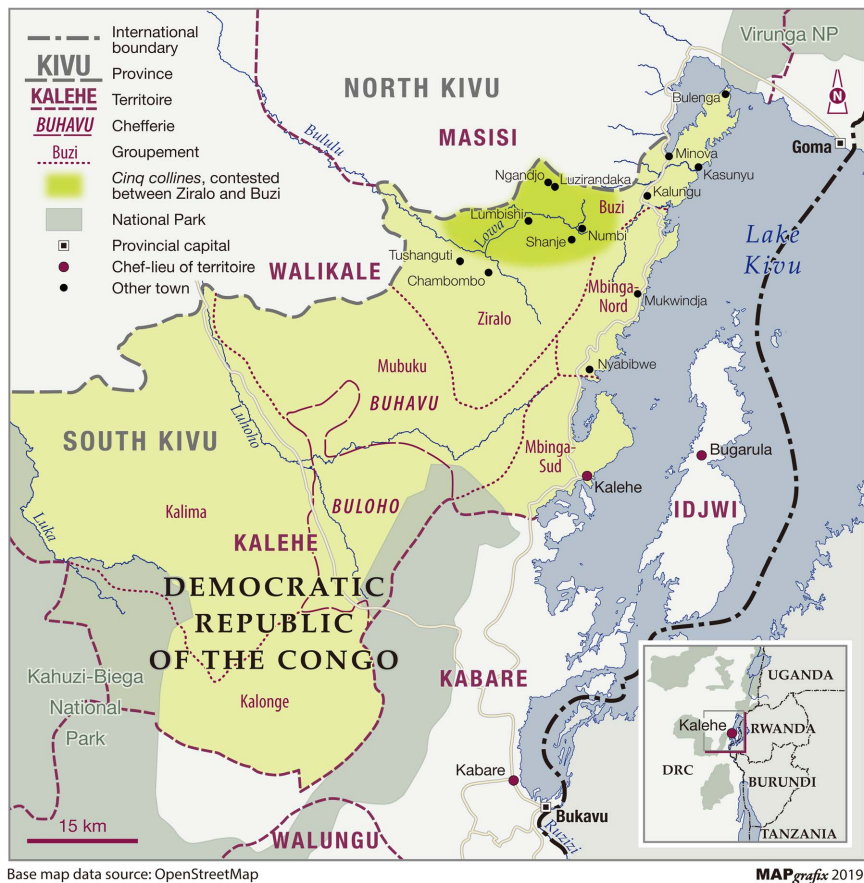


Figure 1. Map of South-Kivu Province [26].

2.1.2. Geotechnical Aspects of the Site

For weight wall material characteristics:

- Repointed masonry see Figure 2;
- The weight by volume is 24 KN/m^3 (Eurocode 6);
- Characteristic compressive strength: $f_{ck} = 25 \text{ N/mm}^2$.

For the material (backfill) supported:

- Soil type: Clean soil with extensive grading: $I_p = 2\%$ (See Appendix);
- Internal angle of friction $\varphi = 40^\circ$;
- Effective cohesion $C' = 0 \text{ KN/m}^2$;
- Backfill weight by volume $\gamma = 17 \text{ KN/m}^3$;
- The slope of the platform $\beta = 0^\circ$;
- The angle of friction δ between the sandy soil and the masonry wall;
- Overloading $q = 10 \text{ KN/m}^2$ (for passengers).

For foundation soil:

- Nature: Loamy soil, not very plastic, coherent and hard with $W_{opt} = 11\%$, $I_p = 2\%$ (Appendix);
- The angle of internal friction $\varphi = 30^\circ$;
- Effective cohesion $C' = 10 \text{ KN/m}^2$;
- Backfill weight by volume $\gamma = 14.3 \text{ KN/m}^3$.

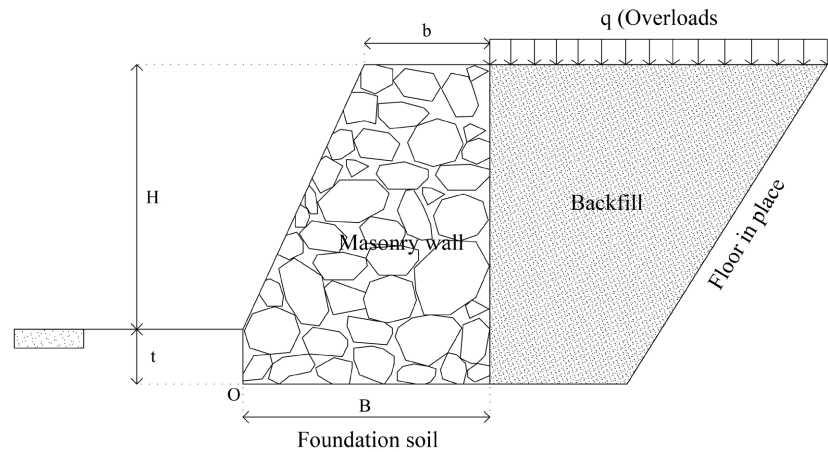


Figure 2. Weight wall.

2.1.3. Determining the Seismic Action of the Study Area

➤ Seismicity zone and peak acceleration

Our study area is located in the territory of Kalehe, more precisely in the city of Nyabibwe. The peak acceleration is taken to be equal to that of the city of Bukavu Equation (1) see **Table 1**.

$$\alpha_{gr} = 0.1239 \times g \quad (1)$$

➤ Determining seismic acceleration coefficients

- Category of importance

According to **Table 2**, in both long-lasting and transitory situations, the importance coefficient $\gamma_i = 1, 2$.

- Soil class, corresponding parameter and safety coefficient

In **Table 3**, we take class D in the sense of NF EN 1998, which corresponds to a soil deposit cohesionless soil of low to medium density or comprising a majority of soft to firm cohesive soils. S describing type 2 spectra. This gives us $S = 1.8$.

According to **Table 4**, the safety factor $r = 1.5$ over the entire height.

- Calculation of seismic acceleration coefficients

By definition, the design horizontal acceleration is

$$\alpha_g = \gamma_i \times \alpha_{gR} \quad (2)$$

Vertical acceleration coefficient

$$K_h = \frac{\alpha_g}{g} \times \frac{S}{r} \quad (3)$$

$$K_h = \frac{\gamma_i \times \alpha_{gR}}{g} \times \frac{S}{r} \quad (4)$$

So $K_h = 0.178416$

Vertical acceleration coefficient

$$K_v = \pm 0.5 \times k_h \quad (5)$$

so $K_v = 0.089208$

Table 1. Peak acceleration (PGA) for PNCR = 10% and TNCR = 475 ans [27].

City	Zone	a_{gR} (g)	City	Zone	a_{gR} (g)
Bujumbura	A	0.1311	Kigali	B	0.1215
Bukavu	B	0.1239	Kigoma	A	0.1353
Bunia	B	0.1169	Kindu	C	0.0332
Butembo	B	0.1157	Kisangani	D	0.0303
Goma	B	0.1266	Lubumbashi	C	0.0523
Kalemie	A	0.1346	Mbuji-Mayi	C	0.0461
Kananga	D	0.0299	Uvira	A	0.1315

Table 2. Coefficients d'importance des accélérations sismiques selon l'EC8 [28].

Category of importance	Description	γ_i
I	Those whose failure presents only a minimal risk to people or economic activity	0.8
II	Those whose failure presents a medium risk to people	1.0
III	Those whose operation is essential for civil protection, defense or the maintenance of public order	1.2
IV	Those whose operation is essential for civil security, defense or the maintenance of public order	1.4

Table 3. S-parameter values in relation to soil class and type of spectrum described [28].

Floor class	Description of stratigraphic profile	S describing type 1 spectra S describing type 2 spectra	S describing type 1 spectra S describing type 2 spectra
A	Rock or similar geological formation with a surface layer of up to 5 m of less resistant material	1.0	1.0
B	Steep deposits of over-consolidated sand, gravel or clay, at least several tens of meters thick, characterized by a progressive increase in mechanical properties with depth	1.2	1.35
C	Deep deposits of medium-density sand, gravel or moderately stiff clay, several tens to several hundreds of meters thick.	1.15	1.5
D	Deposits of cohesionless soils of low to medium density (with or without soft cohesive layers) or comprising mostly soft to firm cohesive soils.	1.35	1.8
E	Soil profile comprising a superficial layer of alluvium with vs values of class C or D and a thickness of between approx. 5 m and 20 m, resting on a stiffer material with vs > 800 m/s	1.4	1.6

Table 4. Values of the r factor for calculating the horizontal seismic coefficient [28].

Type of retaining structure	r
Free-standing gravity walls with displacements up to $dr = 300\alpha S$ (mm)	2
Free-standing gravity walls capable of accepting displacements up to $dr = 200\alpha S$ (mm)	1.5
Reinforced concrete flexural walls, anchored or braced walls, reinforced concrete walls founded on vertical piles, embedded substructure walls and bridge abutments	1

2.2. Characteristics of the Structure

Determining the design values for the mechanical characteristics of the soil

Calculations will be carried out using the ULS in sustainable and accidental (seismic) situations, calculation approach 1.

➤ **Fill soil** $\varphi = 40^\circ$; $C' = 0 \text{ KN/m}^2$; $\delta = 40^\circ$ and $\gamma = 17 \text{ KN/m}^3$ (see soil backfill)

According to Eurocode 7, the partial coefficients: $\gamma_{\varphi'} = 1.25$; $\gamma_{c'} = 1.4$; $\gamma_{\delta} = 1.25$ and $\gamma_{\gamma} = 1.25$ $\phi'_d = 33.8$; $c'_d = 0 \text{ KN/m}^2$; $\delta_d = 33.8$.

➤ **Foundation soil** $\delta'_{fdn} = 30$; $C' = 10 \text{ KN/m}^2$; $\delta_{fdn} = 30$ and $\gamma_{dn} = 14.3 \text{ KN/m}^3$.

According to Eurocode 7, the partial coefficients: $\gamma_{\varphi'} = 1.25$; $\gamma_{c'} = 1.4$; $\gamma_{\delta} = 1.25$ and $\gamma_{\gamma} = 1.00$. $\phi'_{d,fdn} = 24.79$; $c'_d = 7.142 \text{ KN/m}^2$; $\delta_{d,fdn} = 24.79$.

2.2.1. Determining Static Loads

➤ Calculation of deadweight action

The wall acts by its own weight. Starting from the cross-section of the wall $H - t = 4.5 \text{ m}$, $t = 0.6 \text{ m}$,

$$H - t = 4.5 \text{ m} \quad (6)$$

$$b = 0.25 \cdot B \quad (7)$$

the wall volume for a unit length

$$V = 3.4125 \times B \text{ m}^3 \quad (8)$$

with $\gamma_m = 24 \text{ KN/m}^3$, the shares are respectively worth:

$$W = 81.9 \times B \text{ KN} \quad (9)$$

G is the horizontal distance between the axis parallel to the length passing through the wall's center of gravity and the O axis, calculated by barycentric theory applied to elementary surfaces (**Figure 3**).

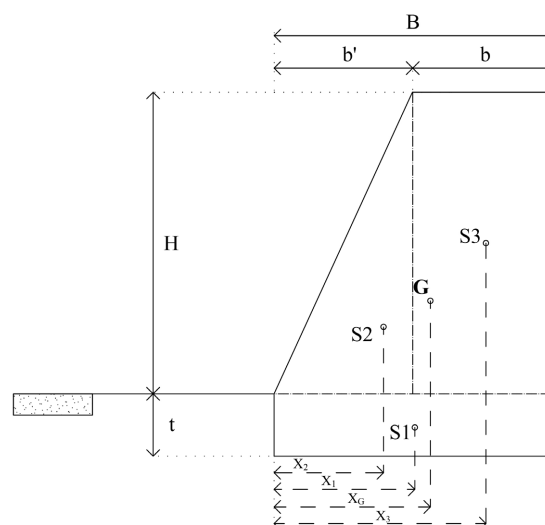


Figure 3. Position of center of gravity.

The moment with respect to the O axis is calculated by the product:

$$M_w = W \times X_G \quad (10)$$

X_G : horizontal distance from the axis parallel to the length passing through the wall's center of gravity to axis O.

For elementary surfaces:

$$S_1 = 0.6 \times B \quad (11)$$

and

$$x_1 = 0.5 \times B \quad (12)$$

$$S_2 = 1.35 \times B \quad (13)$$

and

$$x_2 = 0.4 \times B \quad (14)$$

$$S_3 = 1.8 \times B \quad (15)$$

and

$$x_3 = 0.8 \times B \quad (16)$$

The position of the center of gravity is calculated by:

$$X_G = 0.608 \times B \quad (17)$$

Consequently, the moment with respect to the O axis is then

$$M_w = 49.7952 \times B^2 \text{ KNm} \quad (18)$$

➤ Thrust calculation

The coulomb method for calculating thrust because it gives satisfactory results in practice for weight walls (rough contact between the masonry wall and the ground) having $\delta \geq 0$, $\beta \geq 0$, $\theta \geq 0$. The thrust coefficients exerted by the backfill on the wall are calculated as follows $\phi'_d = 33.8$; $\delta_d = 33.8$; $\beta = 0$ and $\theta = 0$. We have $K_{Ay} = 0.2818$ and $K_{Aq} = 0.2818$.

Calculating backfill thrust for $h = 5.10 \text{ m}$, $\gamma = 17 \text{ KN/m}^3$ and $P_{Ay} = 62.301 \text{ KN/m}$.

Horizontal thrust: $P_{Ahy} = 51.771 \text{ KN/m}$.

Vertical thrust: $P_{Avy} = 34.657 \text{ KN/m}$.

Moment 1 with respect to the o-axis: $M_{Ahy} = 88.0107 \text{ KNm/m}$.

Moment 2 with respect to the o-axis: $M_{Avy} = 34.657 \times B \text{ KNm/m}$.

Calculating overload thrust for $h = 5.10 \text{ m}$ and $q = 10 \text{ KN/m}^3$; $P_{Aq} = 14.3718 \text{ KN/m}$.

Horizontal thrust: $P_{Ahq} = 14.3718 \text{ KN/m}$.

Vertical thrust: $P_{Avq} = 0 \text{ KN/m}$.

Moment about the o-axis: $M_{Ahq} = 36.6480 \text{ KNm/m}$.

Calculation of stop due to foundation soil

The stop will be neglected in the calculation as it acts on the safety side and its durability is not certain, for safety reasons.

2.2.2. Determining Dynamic Loads

The seismic design is also carried out in the ELU, using the Eurocode 7 and 8

methods for accidental design situations. The Mononobe-Okabe method for calculating the total dynamic shear, the Chang and Chen method for calculating the total shear and the Whitman method for calculating the point of application of the dynamic shear.

➤ **Determining total thrust**

This is determined using the Mononobe-Okabe (M-O) method. Total thrust (total active pressure) can be expressed as the superposition of static thrust and dynamic thrust:

$$P_{AE} = \frac{1}{2} \times K_{Ae} \times \gamma \times h^2 (1 - k_v) \quad (19)$$

with $\gamma = 17 \text{ KN/m}^3$; $h = 5.1 \text{ m}$; $q = 10 \text{ KN/m}^3$.

Where the dynamic thrust coefficient,

$$K_{AE} = \frac{\cos^2(\varphi - \theta - \psi)}{\cos\psi \cdot \cos^2\theta \cdot \cos(\delta + \theta + \psi) \left(1 + \sqrt{\frac{\sin(\delta + \varphi) \cdot \sin(\varphi - \beta - \psi)}{\cos(\beta - \theta) \cdot \cos(\delta + \theta + \psi)}} \right)^2} \quad (20)$$

hence

$$\varphi - \beta \geq \psi \quad (21)$$

with

$$\psi = \tanh^{-1} \frac{k_h}{1 - k_v} \quad (22)$$

ψ angle between weight and inertia of corner for $\varphi = \varphi_d = 33.8$;

$\delta = \delta_d = 33.8$; $\beta = 0$; $\theta = 0$,

$$\gamma = \gamma_d \quad (23)$$

(Total density = Dry density);

ψ : angle between the inertia force and the weight of the ground mass;

φ , β , θ and δ : Angles already defined in Coulomb's theory.

Considering the values of K_h and K_v obtained above, we have: $K_h = 0.178416$ and $K_v = 0.089208$.

This implies

$$\psi_1 = \tan^{-1} \frac{k_h}{1 - k_v} \quad (24)$$

So $\psi_1 = 11.08$, $K_h = 0.178416$ and $K_v = -0.089208$.

This implies

$$\psi_2 = \tan^{-1} \frac{k_h}{1 + k_v} \quad (25)$$

So $\psi_2 = 9.30$.

The soil-wall system is considered to undergo an additional rotation, ψ_1 or ψ_2 , depending on whether the vertical component of the seismic acceleration is descending (case 1) or ascending (case 2). In both cases, the condition of equation

20:

Coefficients K_{AE} are then:

$$K_{AE} \approx 0.290, (\psi = 11.08; K_v = 0.089208)$$

$$K_{AE} \approx 0.388, (\psi = 9.30; K_v = -0.089208)$$

In the case of the weight wall in the present study, where there is an overload $q = 10 \text{ KN/m}^3$ on the embankment, the total thrust can be estimated using the Chang & Chen approach (1982):

$$P_{AE} = \frac{1}{2} \times K_{Ae} \times \gamma' \times h^2 (1 - k_v) \quad (26)$$

With

$$\gamma' = \gamma \times \left\{ 1 + \frac{2q}{\gamma \times H_t} \left[\frac{\cos \theta}{\cos(\beta - \theta)} \right] \right\} \quad (27)$$

For the data presented above, we find the following values: $\gamma' = 20.291 \text{ KN/m}^3$; $P_{AE1} = 71.863 \text{ KN/m}$ and $P_{AE2} = 114.983 \text{ KN/m}$;

We therefore retain $P_{AE2} = 114.983 \text{ KN/m}$, the case where the vertical seismic acceleration is upward and the corresponding inertial force is downward. According to Chang & Chen (1982), this thrust is inclined by an angle δ_d ($\delta_d = 33.8$) with respect to the normal to the upstream face of the wall. Its components are then: $P_{AEh} = 95.549 \text{ KN/m}$ and $P_{AEv} = 63.964 \text{ KN/m}$.

➤ **Determining the static and dynamic components of total thrust**

$$P_{Ah} = 66.142 \text{ KN/m} \text{ and } P_{Av} = 34.657 \text{ KN/m}$$

The dynamic components of total thrust can be derived from the following expressions:

$$\Delta P_{AEh} = 29.407 \text{ KN/m} \text{ and } \Delta P_{AEv} = 29.307 \text{ KN/m}$$

➤ **Determining their respective points of application**

- 1) Point of application of horizontal static thrust P_{Ah} : $y_1 = 1.884 \text{ m}$.
- 2) Point of application of vertical static thrust P_{Av} : $y_2 = 1.7 \text{ m}$.
- 3) Point of application of horizontal dynamic thrust: According to Whitman (1998), the point of application of the dynamic thrust ΔP_{AE} of an unloaded fill on a weight wall is at

$$y_i = 0.6 \times h \quad (28)$$

- 4) So, in the case of an overloaded embankment, we propose the formula:

$$y_i = 0.6 \times (H_t + h_q) \quad (29)$$

with

$$h_q = \frac{q}{\gamma} \quad (30)$$

In the case of this study, $h = 5.1 \text{ m}$; $q = 10 \text{ KN/m}^2$; $\gamma = 17 \text{ KN/m}^3$ hence $y_3 = 3.412 \text{ m}$ with $h_q = 0.588 \text{ m}$.

- 5) Point of application (horizontal dynamic thrust ΔP_{AEv}): $y_4 = 3.060 \text{ m}$

➤ **Determination of inertia effects on wall weight**

Figure 4 shows the coordinates of the wall's center of gravity for seismic design.

We have $Y_{G1} = 0.3$ m; $Y_{G2} = 2.1$ m and $Y_{G3} = 2.85$ m. Hence $Y_G = 2.172$ m.

2.3. Design Principle in Accordance with Eurocode

The components used in the pointed masonry retaining wall are of various types and origins. It is built of rubble stone and cement mortar (pozzolanic type CEM IV/B class 32.5, grey in color and produced in Uganda).

Weight walls are the most common type of retaining structure, and for this reason several approaches have been developed that focus on their dimensioning [29]. Weight walls are usually dimensioned using one of two approaches: one based on seismic lateral pressures or the other based on the permanent displacement of the structure. The first approach, which is commonly used, consists in applying the M-O method, adopting the same value of pseudo-static acceleration for the inertia forces of the active corner and all the masses of the structure. Eurocode 8 [28] (NF EN 1998-5-7.3.2.2 clause (4)) proposes, in the absence of specific studies, to calculate the horizontal (k_h) and vertical (k_v) seismic coefficients affecting all masses.

$$k_h = \alpha \times \frac{s}{r} \quad (31)$$

$$k_v = \pm 0.5 \cdot k_h \quad (32)$$

(if $\frac{a_{vg}}{a_g}$ is greater than 0.6)

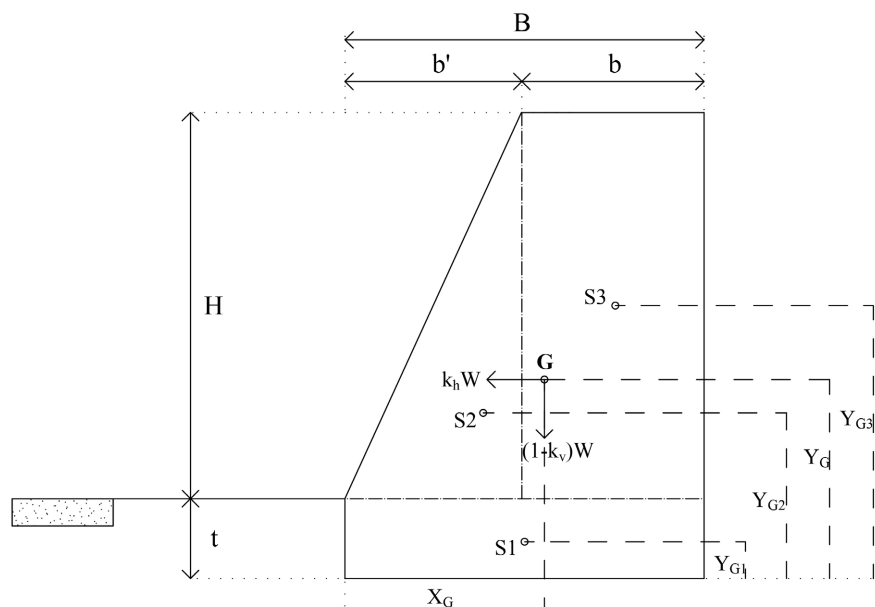


Figure 4. Determining the coordinates of the wall's center of gravity for seismic design.

$$k_v = \pm 0.33 \cdot k_h \quad (33)$$

(if $\frac{a_{vg}}{a_g}$ is less or equal to 0.6).

a_{vg} : Vertical component of the design acceleration a_g .

r : safety factor, which takes on the values indicated according to the type of retaining structure. For walls less than 10 m high, the seismic coefficient must be assumed to be constant over the entire height. It is given in accordance with NF EN 1998-5.

S : characteristic parameter of the soil class defined in standard NF EN 1998-1-3.2.2.2, involved in determining the shape of the soil's elastic response spectrum.

$$\alpha = \frac{\alpha_g}{g} \quad (34)$$

(α ratio of the design acceleration a_g for class A soil to the acceleration g of gravity) with

$$\alpha_g = \gamma_i \times \alpha_{gR} \quad (35)$$

α_{gR} : Accélération maximale de référence (PGA);

γ_i : Coefficients d'importance des accélérations sismiques selon l'EC8 (NF EN 1998).

The design values for the effects of actions E_d and resistances R_d and their combinations in seismic situations are determined in accordance with Eurocode 0 (EN 1990) [30] and Eurocode 7 [31] (EN 1997). Calculations focus on reliability in relation to the “non-collapse” requirement (ultimate limit state) and the “damage limitation” requirement (service limit state). The various values of the partial coefficients are given in Eurocode 7 (EN 1997-1). Partial factors for actions (and their effects) should normally be equal to 1.0 in accidental situations (EN 1997-1-2.4.7.1). However, the use of one approach or another for each type of structure also depends on one country or another in the Euro zone. In the case of the Democratic Republic of Congo, approach 1 could be used in the calculations.

✧ Verification of sliding stability

The general stability equation for the sliding stability of the wall on its base becomes:

$$V_{Ed} \leq V_{Rd} + R_{pd} \quad (36)$$

V_{Ed} : Design value of the horizontal load (or horizontal shear force) resulting from the weighted horizontal actions acting on the wall. In the case of **Figure 5**, this is:

$$V_{Ed} = (k_h \cdot W)_d + (P_{AE})_d \cdot \cos(\delta_d + \theta) + U_d \cdot \cos \theta \quad (37)$$

$(P_{AE})_d$: dynamic thrust calculation value total land;

U_d : calculation value for the resultant of hydrostatic and hydrodynamic thrusts;

B : design width (base) of the weight wall's surface foundation.

The bearing capacity of the subsoil q_{Rd} can be calculated using known relationships, considering the excess caused by the intensity, inclination and eccentricity of the seismic action.

✧ **Checking rollover stability**

Verification of overturning stability consists in ensuring that the resultant of the destabilizing moments $M_{Ed,dst}$ in relation to the downstream lower edge (point 'O' in **Figure 5**) is less than or equal to the resultant of the stabilizing moments $M_{Ed,stab}$ with respect to the same edge:

$$M_{Ed,dst} \leq M_{Ed,stab} \quad (44)$$

- ✚ The forces that cause the destabilizing moments, in relation to **Figure 5**, are:
 - The horizontal component of total dynamic thrust: $(P_{AE})_d \cdot \cos(\delta_d + \theta)$;
 - The horizontal component of the resultant of hydrostatic and hydrodynamic thrusts: $U_a \cdot \cos \theta$ (for a vertical wall, $\theta = 0^\circ$ ($\cos \theta = 1$));
 - The horizontal inertia force due to the weight of the wall: $(k_h \cdot W)_d$;
 - Lifting force due to water pressure under the base: U_{Rd}
- ✚ The forces that contribute to the stabilizing moments, on the other hand, are:
 - The vertical component of total dynamic thrust: $(P_{AE})_d \cdot \sin(\delta_d + \theta)$;
 - The vertical component of the resultant of hydrostatic and hydrodynamic thrusts: $U_d \cdot \cos \theta$;
 - The resultant of the wall's weight and vertical inertia force: $(1 - k_v) \cdot W_d$;
 - The resultant of the total stop, if any: $(P_{PE})_d$.

✧ **Verification of the structure's internal (structural) stability**

The study of the structural stability of load-bearing walls is a question of material strength and is specific to each type of wall in terms of the forces (and displacements) acting on it. The stability of concrete and reinforced concrete load-bearing walls is assessed in relation to the provisions of Eurocode 2 [32] whereas the provisions of Eurocode 6 apply to masonry walls [33].

3. Results

3.1. Pre-Sizing

The complete calculation of a retaining wall is a rather laborious task, since the dimensioning of the structure and its verification require a succession of long and iterative calculations. To achieve the right results as quickly as possible, it's important to pre-dimension the wall's geometric characteristics as accurately as possible.

The selected site leads us to consider the following values according to **Figure 6**:

- A useful height of $H = 4.5$ m;
- A plug in the ground $t = 0.6$ m;
- Free height $h = 5.1$ m;

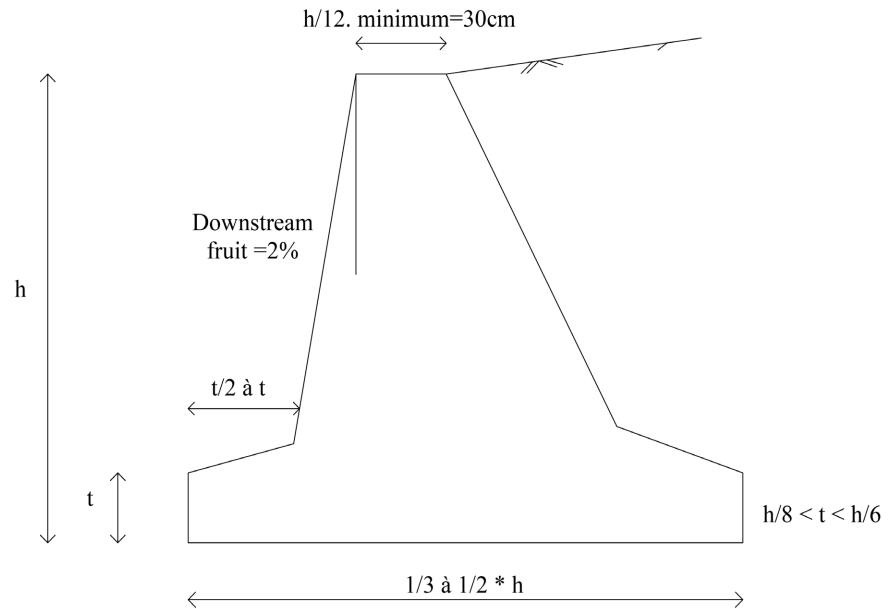


Figure 6. Weight wall pre-dimensioning [34].

➤ A top width b : From **Figure 6**, we have:

$$b = \frac{h}{12} \quad (45)$$

With

$$h = 12b \quad (46)$$

$B \in \left[\frac{h}{3}; \frac{h}{2} \right]$ Considering

$$B = \frac{h}{3} \quad (47)$$

with

$$h = 3 \times B \quad (48)$$

(1) and (2), we have

$$12 \times b = 3 \times B \quad (49)$$

The wall is equipped with a network of barbicans for rapid evacuation of seepage water into the backfill.

3.2. Static Dimensioning of the Structure ($K_h = 0$ and $K_v = 0$)

✚ Verification of sliding stability

The destabilizing actions are $P_{Ah\gamma}$ and P_{Ahq} . They are weighted by unfavorable partial coefficients $\gamma_G = 1.35$ and $\gamma_Q = 1.50$. Hence, $H_{Ed} = 91.44855$ KN/m

The stabilizing actions are $P_{Av\gamma}$ and W . They are all permanent and weighted by favourable partial coefficients $\gamma_{G,fav} = 1.00$ and the partial resistance coeffi-

cient is equal to $\gamma_{Rh} = 1.00$. So

$$H_{Rd} = 16.00 + 37.825B \text{ KN/m} \quad (50)$$

The stability condition

$$H_{Rd} \geq H_{Ed} \quad (51)$$

Hence $B \geq 1.994 \text{ m}$.

✚ Checking rollover stability

The destabilizing actions are $M_{Ah\gamma}$ and M_{Ahq} . They are weighted by unfavorable partial coefficients $\gamma_G = 1.35$ and $\gamma_Q = 1.50$. Hence $M_{Ed} = 173.786 \text{ KNm/m}$.

The stabilizing actions are $M_{Av\gamma}$ and M_{W} . They are all permanent and weighted by favourable partial coefficient $\gamma_{G, fav} = 1.00$. So

$$M_{Rd} = 34.657B + 49.7952B^2 \text{ KNm/m} \quad (52)$$

The stability condition requires that

$$M_{Rd} \geq M_{Ed} \quad (53)$$

The roots of this inequation are $B_1 = -2.24 \text{ m}$ and $B_2 = 1.55 \text{ m}$.

The solution to this inequation is $B \geq 1.55 \text{ m}$.

✚ Verification of punching stability

$$N = 46.786 + 110.565B \quad (54)$$

$$N_{Rd} = 46.786 + 110.565B \text{ KN/m} \quad (55)$$

The resultant of the moments is

$$\Delta M = 49.7952B^2 + 34.657B - 173.7860 \quad (56)$$

Load eccentricity e_B with respect to the axis passing through the center of the footplate:

$$e_B = \frac{B}{2} - \frac{\Delta M}{N} \quad (57)$$

$$e_B = 0.5 \times B - \frac{\Delta M}{N} \quad (58)$$

In this case, check that the eccentricity is in the middle third

$$|e_B| \leq \frac{B}{6} \quad (59)$$

The fictitious cross-section of the wall base for a unit length is:

$$B' = B - 2e_B \quad (60)$$

and

$$L' = 1 \text{ m} \quad (61)$$

or

$$A' = B' \times L' \quad (62)$$

so

$$A' = B - 2e_B \quad (63)$$

The average stress exerted by the wall under the various loads is:

$$q_{Ed} = \frac{N_{Ed}}{A'} \quad (64)$$

this implies

$$q_{Ed} = \frac{46.786 + 110.565B}{(B - 2)e_B} \quad (65)$$

The load-bearing capacity (ultimate stress) is calculated as follows:

➤ **Determination of load-bearing capacity factors in drained condition N_q , N_c and N_γ**

The formulas below are proposed by Eurocode 7, but other relationships are also accepted: $\delta_{d,fdn} = 24.79^\circ = \phi'_{d,fdn}$; $N_q = 10.428$; $N_c = 20.143$; $N_\gamma = 8.708$.

➤ **Determination of resultant inclination factors in drained condition i_q , i_c and i_γ**

Eurocode 7 defines three factors that take into account the inclination of the load resultant R with respect to the vertical. For very long walls: $L' = \infty$ m; so $m_B = 2$.

$$H_{Ed} = 91.44588 \text{ KN/m and}$$

$$N_{Ed} = 34.786 + 110.565B \quad (66)$$

$$A' = B' \times 1 \quad (67)$$

so

$$A' = (B - 2e_B) \cdot m^2 \quad (68)$$

After replacing the numerical values, the coefficients respectively take on the following expressions:

$$i_q = \left[1 - \frac{91.44855}{46.786 + 183.748B - 146.366e_B} \right]^2 \quad (69)$$

$$i_c = 1.106 \cdot i_q - 0.1060 \quad (70)$$

$$i_\gamma = \left[1 - \frac{91.44855}{46.786 + 183.748B - 146.366e_B} \right]^3 \quad (71)$$

It goes without saying that the coefficients $i_q(B)$, $i_c(B)$ and $i_\gamma(B)$ are a function of and cannot be calculated directly. The ultimate load-bearing capacity can then be deduced from the relationship:

$$q_{ult} = \left(N_\gamma \times i_\gamma \times \gamma_{fdn} \times \frac{B'}{2} \right) + \left(N_q \times i_q \times \gamma_{fdn} \times t \right) + \left(N_c \times i_c \times C'_{d,fdn} \right) \quad (72)$$

$$N_\gamma = 8.708; N_c = 20.413; N_q = 10.428; \gamma_{fdn} = 14.3 \text{ KN/m}^3;$$

$$C'_{d,fdn} = 33.8 \text{ KN/m}^2 \text{ and } t = 0.6 \text{ m.}$$

Expression becomes:

$$q_{ult} = (79.6782 \times i_\gamma \times B') + (89.47224 \times i_q) + (689.9594 \times i_c) \quad (73)$$

With the partial resistance coefficient $\gamma_{Rv} = 1.0$; we find:

$$q_{Rd} = \frac{q_{ult}}{\gamma_{Rv}} \tag{74}$$

$$q_{Rd} = q_{ult} \tag{75}$$

Punching stability means ensuring that:

$$q_{Ed} \leq q_{Rd} \tag{76}$$

The solution to this inequality is more complex than previous inequalities, given the dependence of several parameters on the variable B. It is therefore solved by iteration. The results are shown in **Table 5**, where the variable is the base width B. The objective is to determine the value of B that satisfies the stability condition

$$q_{Ed} \leq q_{Rd} \tag{77}$$

and the condition of the central third

$$|e_B| \leq \frac{B}{6} \tag{78}$$

From the results in **Table 5** and **Figure 7**, it can be seen that punching stability is already achieved for $B \geq 3.1$ m where $B_{min} = 3.1$ m where:

$$q_{Ed} \leq q_{Rd} \tag{79}$$

$$\frac{q_{Ed}}{q_{Rd}} = 29.147\% \tag{80}$$

$$e_B \leq e_{lim} = \frac{B}{6} \tag{81}$$

$$\frac{e_B}{e_{lim}} = 95.145\% \tag{82}$$

Table 5. Summary of seismic calculation of weight wall based on punching stability (load-bearing capacity).

B (m)	N _{ed} (KN)	ΔM (KNm)	ΔM/N _{ed}	e (m)	B/6	B' (m)	A' (m ²)	q _{Ed} (kN/m ²)	i _q	i _c	i _v	q _{Rd} (kN/m ²)	q _{Ed} /q _{Rd} (%)
0	46.786	-173.789	-3.71455	3.7146	0	-7.4291	-7.4291027	-6.297665	1.402	1.4446	1.65996	139.526209	-4.5136072
0.5	102.07	-144.012	-1.41093	1.6609	0.083	-2.8219	-2.8218637	-36.170598	3.518	3.7847	6.59787	1442.53993	-2.5074244
1	157.35	-89.3368	-0.56775	1.0678	0.167	-1.1355	-1.1355098	-138.573	0.054	-0.047	-0.0124	-26.275563	527.383565
1.5	212.63	-9.7643	-0.04592	0.7959	0.25	-0.0918	-0.0918416	-2315.22	0.309	0.2358	0.17177	189.058334	-1224.6062
2	267.92	94.7058	0.353491	0.6465	0.333	0.707	0.7069813	378.957693	0.51	0.4577	0.36386	381.892898	99.2314064
2.5	323.2	224.074	0.6933	0.5567	0.417	1.3866	1.3865999	233.087068	0.616	0.575	0.48311	505.16003	46.1412333
3	378.48	378.339	0.999624	0.5004	0.5	1.9992	1.9992486	189.311627	0.682	0.6481	0.56303	597.878433	31.6638996
3.1	389.54	412.18	1.058126	0.4919	0.517	2.1163	2.1162511	184.069607	0.692	0.6596	0.57598	614.185384	29.9697147
3.2	400.59	447.016	1.115884	0.4841	0.533	2.2318	2.2317671	179.496331	0.702	0.6704	0.58813	629.921773	28.4950193
3.3	411.65	482.849	1.172958	0.477	0.55	2.3459	2.3459164	175.47535	0.711	0.6804	0.59957	645.142429	27.1994744

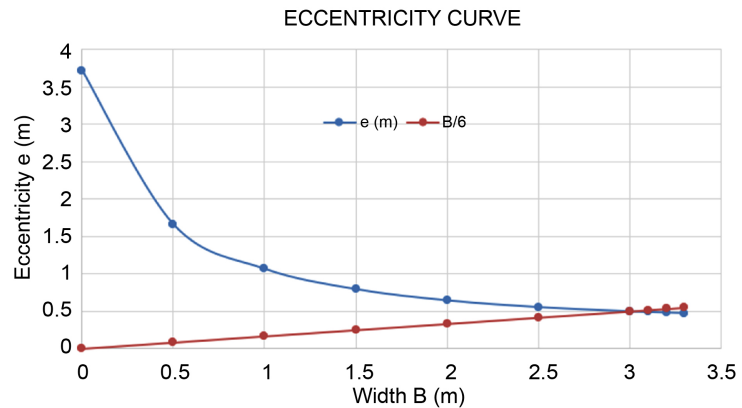


Figure 7. Eccentricity curves.

➤ Interpretation of results

After verification of the three main stability criteria, the minimum dimensions found for the width of the footing (base) are:

- 1) Sliding stability: $B \geq 1.9945$ m;
- 2) Rollover stability: $B \geq 1.55$ m;
- 3) Punching stability: $B \geq 3.1$ m.

Hence, the static dimensioning gives the following geometric dimensions for the wall:

Sole width: $B = 3.1$ m;

Width of small base: $b = 0.775$ m and Actual wall weight: $W = 253.89$ KN/m.

3.3. Dynamic (Seismic) Dimensioning of the Structure

$$K_h = 0.178416 \text{ and } K_v = 0.089208$$

Checking stability criteria: Unlike static design, seismic design is based on accidental (non-permanent) project situations. Consequently, the partial coefficients of actions and their effects are taken to be equal to 1.0 (EN 1997-1 2.4.7.1(3)).

✚ Verification of sliding stability

❖ Destabilizing actions are:

The horizontal component of static thrust: $P_{Ah} = 66.142$ KN/m ;

The horizontal component of dynamic thrust: $\Delta P_{AEh} = 29.407$ KN/m ;

The horizontal inertia force due to the weight of the wall:

$$F_h = 14.612B \quad (83)$$

So

$$H_{Ed} = P_{Ah} + \Delta P_{AEh} + F_h \quad (84)$$

this implies

$$H_{Ed} = 95.549 + 14.612B \quad (85)$$

❖ The stabilizing actions are:

The vertical component of static thrust: $P_{Av} = 34.657$ KN/m ;

The vertical component of dynamic thrust: $\Delta P_{AEv} = 29.307$ KN/m ;

The resultant of the wall's weight and vertical inertia force:

$$W + F_v = (1 + k_v)w \quad (86)$$

So

$$H_{Rd} = \frac{\gamma_{G,fav} \times (P_{Av} + \Delta P_{AEv} + W + F_v) \times \tan(\delta_{d,fdn})}{\gamma_{Rh}} \quad (87)$$

$$\gamma_{G,fav} = \gamma_{Rh} = 1.0 \quad \text{and} \quad \delta_{d,fdn} = 24.79^\circ$$

This implies

$$H_{Rd} = 29.541 + 41.200B \quad (88)$$

The stability condition requires that:

$$H_{Rd} \geq H_{Ed} \quad (89)$$

The solution to the inequality is: $B \geq 2.482$ m.

🚧 Checking rollover stability

Rollover stability is verified by the balance of moments around point o.

The moment of static thrust P_{Ah} : $M_{Ah} = 118.923$ KNm .

The moment of dynamic thrust ΔP_{AEh} : $\Delta M_{AEh} = 95.161$ KNm .

The moment of inertia of the wall F_h :

$$M_{Fh} = F_h \times \gamma_G \quad (90)$$

hence

$$M_{Fh} = 34.875 \times B \quad (91)$$

So

$$\begin{aligned} M_{Ed} &= M_{Ah} + \Delta M_{AEh} + M_{Fh} \\ M_{Ed} &= 214.084 + 34.875 \times B \end{aligned} \quad (92)$$

The stabilizing actions are:

The moment of vertical static thrust P_{Av} :

$$M_{Av} = P_{Av} \times B \quad (93)$$

$$M_{Av} = 34.657 \times B \quad (94)$$

The moment of dynamic thrust ΔP_{AEv} :

$$\Delta M_{AEv} = \Delta P_{AEv} \times B \quad (95)$$

$$\Delta M_{AEv} = 29.307 \times B \quad (96)$$

The moment of resultant weight and vertical force of inertia:

$$M_{Rw} = 54.237B^2 \quad (97)$$

So

$$\begin{aligned} M_{Rd} &= M_{Av} + M_{RW} \\ M_{Rd} &= 63.964 \times B + 54.237 \times B^2 \end{aligned} \quad (98)$$

The stability condition requires that

$$M_{Rd} \geq M_{Ed} \quad (99)$$

The roots of this inequation are $B_1 = -2.2719$ m and $B_2 = 1.7366$ m.

The solution is $B \geq 1.7366$ m.

✚ Verification of punching stability

The resultant of the vertical loads acts unfavorably with respect to punching stability, and is therefore equal to:

$$N_{Ed} = 63.964 + 89.206 \times B \quad (100)$$

The resultant of the moments is:

$$\Delta M = 54.237 \times B^2 + 29.089 \times B - 214.084 \quad (101)$$

The eccentricity of load e_B with respect to the axis passing through the center of the footing:

$$e_B = 0.5B - \frac{\Delta M}{N} \quad (102)$$

In this case, check that the eccentricity is in the middle third:

$$|e_B| \leq \frac{B}{6} \quad (103)$$

The fictitious cross-section of the wall base for a unit length is:

$$B' = B - 2e_B \quad (104)$$

$$L' = 1 \text{ m}$$

so

$$A' = B' \times L' \quad (105)$$

And

$$A' = B - 2 \times e_B \quad (106)$$

The average stress exerted by the wall under the various loads is:

$$q_{Ed} = \frac{N_{Ed}}{A'} \quad (107)$$

The load-bearing capacity (ultimate stress) is calculated as follows:

➤ Determination of load-bearing capacity factors in drained condition N_q ,

N_c , N_γ

Bearing capacity factors in drained condition: $N_q = 10.428$; $N_c = 20.413$; $N_\gamma = 8.708$.

➤ Determination of resultant inclination factors in drained condition i_ϕ , i_c and i_γ

The load inclination factors become: $m_B = 2$;

$$H_{Ed} = 95.549 + 14.612 \times B \quad (108)$$

$$N_{Ed} = 63.961 + 89.206 \times B \quad (109)$$

$$A' = B - 2 \times e_B \quad (110)$$

$$c'_{d,fdn} = 7.142 \text{ KN/m}^2$$

$$\phi_{d,fdn} = 24.79^\circ$$

$$i_q = \left[1 - \frac{95.549 + 14.612B}{63.961 + 104.669B - 30.927e_B} \right]^2 \tag{111}$$

$$i_c = 1.106i_q - 0.106 \tag{112}$$

$$i_\gamma = \left[1 - \frac{164.009 + 14.612B}{109.794 + 104.669B - 30.927e_B} \right]^3 \tag{113}$$

The ultimate load-bearing capacity can then be deduced from the relationship:

$$q_{ult} = (62.2622 \times i_\gamma \times B') + (89.472 \times i_q) + (145.789 \times i_c) \tag{114}$$

With the partial resistance coefficient $\gamma_{Rv} = 1.0$; we find:

$$q_{Rd} = \frac{q_{ult}}{\gamma_{Rv}} \tag{115}$$

$$q_{Rd} = q_{ult} \tag{116}$$

Punching stability means ensuring that:

$$q_{Ed} \leq q_{Rd} \tag{117}$$

Using the same procedure as for the static calculation, the results are presented in **Table 6**, where the only variable is the width of the footing (base).

From the results in **Table 6** and **Figure 8**, it can be seen that punching stability is already achieved for $B \geq 3.40$ m where $B_{min} = 3.40$ m.

$$q_{Ed} \leq q_{Rd} \tag{118}$$

$$\frac{q_{Ed}}{q_{Rd}} = 87.6788\% \tag{119}$$

and

$$e_B \leq e_{lim} = \frac{B}{6} \tag{120}$$

$$\frac{e_B}{e_{lim}} = 92.3133\% \tag{121}$$

Assessing the impact of seismic action: Interpreting the results

1) Sliding stability: $B \geq 2.482$ m;

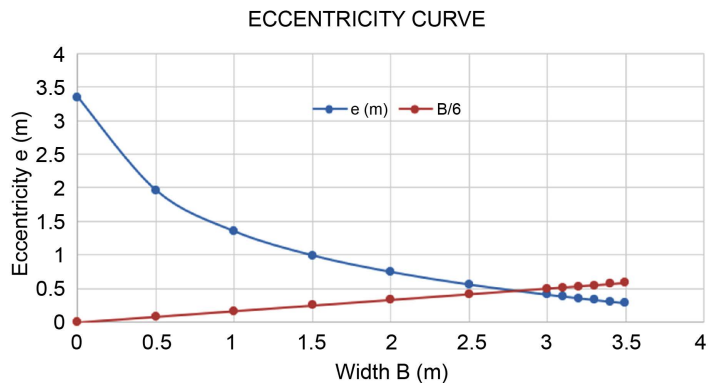


Figure 8. Eccentricity curves.

Table 6. Summary of weight wall seismic calculation based on punching stability (load-bearing capacity).

B (m)	N _{ed} (KN)	ΔM (KNm)	ΔM/N _{ed}	e (m)	B/6	B' (m)	A' (m ²)	Q _{Bd} (kN/m ²)	i _q	i _c	i _y	Q _{Rd} (kN/m ²)	Q _{Bd} /Q _{Rd} (%)
0	63.964	-214.084	-3.346945	3.3469452	0	-6.693890	-6.693890	-9.555579	11.669663	12.800647	39.864606	-13704.32	0.0697268
0.5	108.567	-185.98025	-1.713045	1.9630459	0.0833333	-3.426091	-3.426091	-31.68829	0.7230612	0.6937057	-0.614840	296.98373	-10.670044
1	153.17	-130.758	-0.853678	1.3536789	0.1666667	-1.707357	-1.707357	-89.71171	0.0171614	-0.087019	0.0022482	-11.39000	787.63517
1.5	197.773	-48.41725	-0.244812	0.9948122	0.25	-0.489624	-0.489624	-403.9279	0.1462342	0.055735	0.0559208	19.504666	-2070.9297
2	242.376	61.042	0.2518484	0.7481516	0.3333333	0.5036967	0.5036967	481.1943	0.2512365	0.1718676	0.1259286	51.484323	934.64238
2.5	286.979	197.61975	0.6886209	0.5613791	0.4166667	1.3772419	1.3772419	208.37226	0.3266743	0.2553017	0.1867121	82.458961	252.69813
3	331.582	361.316	1.0896731	0.4103269	0.5	2.1793463	2.1793463	152.14746	0.3824394	0.316978	0.236507	112.52137	135.2165
3.1	340.5026	397.30947	1.1668324	0.3831676	0.5166667	2.3336648	2.3336648	145.90896	0.391868	0.327406	0.2453069	118.43627	123.19617
3.2	349.4232	434.38768	1.2431564	0.3568436	0.5333333	2.4863128	2.4863128	140.53871	0.4008209	0.3373079	0.2537614	124.32114	113.04491
3.3	358.3438	472.55063	1.3187074	0.3312926	0.55	2.6374149	2.6374149	135.86933	0.4093329	0.3467222	0.2618876	130.177	104.37277
3.4	367.2644	511.79832	1.3935419	0.3064581	0.5666667	2.7870837	2.7870837	131.77372	0.4174354	0.3556835	0.2697018	136.00487	96.888973
3.5	376.185	552.13075	1.4677107	0.2822893	0.5833333	2.9354214	2.9354214	128.15366	0.425157	0.3642237	0.2772197	141.80574	90.372693

2) Rollover stability: $B \geq 1.7366$ m;

3) Punching stability: $B \geq 3.4$ m.

Hence, the static dimensioning gives the following geometric dimensions for the wall:

- Width of sole (large base): $B = 3.4$ m;
- Width of small base: $b = 0.85$ m;

Actual wall weight (per meter length): $W = 278.46$ KN/m².

A comparison of the minimum dimensions for the two sizing approaches is shown in **Table 7**.

3.4. Discussion

The two design methods show a difference of 24.47% in slip stability, 12.038% in tilt stability and 9.677% in punching stability. This difference is substantial and demonstrates the impact of earthquakes on gravity wall design in this study. The tilting stability condition is the highest and most dangerous. The article by P. A. Yadav *et al.* (2018) [6] presents the results of evaluation of retaining walls stability under static and seismic loads. Studies have shown that for slender walls with low backfill heights, the pseudo-static Mononobe-Okabe method provides results close to more rigorous dynamic analyses.

3.5. Limits

In this work, it is assumed that the natural climatic conditions corresponding to the exposure environment of these materials generally vary and thus produce certain thermal effects that may be characterized by a longer stabilization time.

Table 7. Comparison of footing widths and wall unit weights for the two dimensioning approaches.

Values	Slide	Turnaround	Punching
<i>Bmin, statique</i> (m)	1.994	1.55	3.1
<i>Bmin, stsmique</i> (m)	2.482	1.7366	3.4
<i>Wmin, statique</i> (kN/m)	163.3086	126.945	253.89
<i>Wmin, stsmique</i> (kN/m)	203.2758	142.22754	278.46
<i>Bmin, sism/Bmin, stat</i>	1.244	1.120	1.096
<i>Wmin, sism/Wmin, stat</i>	1.244	1.120	1.096
$\Delta Bmin/Bmin, stat$	24.47%	12.038%	9.677%

4. Conclusions

The overall objective of this thesis is to contribute to the current state of knowledge on the study of stability of retaining structures under dynamic loading in order to analyze its effects on retaining structures in South Kivu. In Nyabibwe, South Kivu, an application of grouted masonry gravity wall was proposed. In Nyabibwe, the difference was 24.47% in slip stability, 12.038% in overturning stability and 9.677% in punching shear stability. This is a huge value that shows the actual effects of the earthquake on the construction of the bearing wall at the selected sites. For the structure studied, *i.e.* the load-bearing wall supporting a road embankment, it was found that the effects of seismic loads are significant compared to the purely static loads.

It was found that the effects of seismic loads are significant compared to purely static loads on the structure under investigation, *i.e.* the grouted masonry wall supporting a road embankment.

Conflicts of Interest

The authors declare no conflicts of interest regarding the publication of this paper.

References

- [1] Anderson, D., *et al.* (2008) Seismic Analysis and Design of Retaining Walls, Buried Structures, Slopes and Embankments. NCHRP (National Cooperative Highway Research Program) Report 611, Transportation Research Board, USDOT, Washington DC.
- [2] Seman, M.A., Syed Mohsin, S.M. and Jaini, Z.M. (2019) Blast Load Assessment: RC Wall Subjected to Blast Load. *IOP Conference Series Earth and Environmental Science*, **244**, 012007. <https://doi.org/10.1088/1755-1315/244/1/012007>
- [3] Chen, Y., Song, J., Zhong, S., Liu, Z. and Gao, W. (2021) Effect of Destructive Earthquake on the Population-Economy-Space Urbanization at County Level—A Case Study on Dujiangyan County, China. *Sustainable Cities and Society*, **76**, Article ID: 103345. <https://doi.org/10.1016/j.scs.2021.103345>
- [4] Tiwari, R. and Lam, N. (2021) Modelling of Seismic Actions in Earth Retaining Walls and Comparison with Shaker Table Experiment. *Soil Dynamics and Earth-*

- quake Engineering*, **150**, Article ID: 106939.
<https://doi.org/10.1016/j.soildyn.2021.106939>
- [5] Kramer, S.L. (1996) Geotechnical Earthquake Engineering. Prentice Hall International Series in Civil Engineering and Engineering Mechanics, Upper Saddle River, 643.
- [6] Yadav, P.A., Singh, D.K., Dahale, P.P. and Padade, A.H. (2018) Analysis of Retaining Wall in Static and Seismic Condition with Inclusion of Geofoam Using PLAXIS 2D. In: Latha Gali, M. and Raghuvver Rao, P., Eds., *Geohazards. Lecture Notes in Civil Engineering*, vol 86. Springer, Singapore, 223-240.
https://doi.org/10.1007/978-981-15-6233-4_16
- [7] Annapareddy, V.R. and Pain, A. (2019) Effect of Strain-Dependent Dynamic Properties of Backfill and Foundation Soil on the External Stability of Geosynthetic Reinforced Waterfront Retaining Structure Subjected to Harmonic Motion. *Applied Ocean Research*, **91**, Article ID: 101899. <https://doi.org/10.1016/j.apor.2019.101899>
- [8] Nandi, R. and Choudhury, D. (2023) Analytical Method for Determining Displacement and Bending Moment of Embedded Cantilever Retaining Walls Subjected to Pseudo-Static Earthquake Accelerations. *Soil Dynamics and Earthquake Engineering*, **164**, Article ID: 107642. <https://doi.org/10.1016/j.soildyn.2022.107642>
- [9] Callisto, L., et al. (2010) Seismic Design of Flexible Cantilevered Retaining Walls. *Journal of Geotechnical and Geoenvironmental Engineering*, **136**, 344-354.
[https://doi.org/10.1061/\(ASCE\)GT.1943-5606.0000216](https://doi.org/10.1061/(ASCE)GT.1943-5606.0000216)
- [10] Rahbari, P., Ravichandran, N. and Juang, C.H. (2017) Seismic Geotechnical Robust Design of Cantilever Retaining Wall Using Response Surface Approach *Journal of GeoEngineering*, **12**, 147-155.
- [11] Kilic, I.E., Cengiz, C., Edincliler, A. and Guler, E. (2021) Seismic Behavior of Geosynthetic-Reinforced Retaining Walls Backfilled with Cohesive Soil. *Geotextiles and Geomembranes*, **49**, 1256-1269. <https://doi.org/10.1016/j.geotxm.2021.04.004>
- [12] Sam, M.B. Helwany, M.B. and Budhu, M. (2001) Seismic Analysis of Segmental Retaining Walls. I: Model Verification. *Journal of Geotechnical and Geoenvironmental Engineering*, **127**, 741-749.
[https://doi.org/10.1061/\(ASCE\)1090-0241\(2001\)127:9\(741\)](https://doi.org/10.1061/(ASCE)1090-0241(2001)127:9(741))
- [13] Cakir, T. (2013) Evaluation of the Effect of Earthquake Frequency Content on Seismic Behavior of Cantilever Retaining Wall Including Soil-Structure Interaction. *Soil Dynamics and Earthquake Engineering*, **45**, 96-111.
<https://doi.org/10.1016/j.soildyn.2012.11.008>
- [14] Papazafeiropoulos, G., Psarropoulos, P. and Tsompanakis, Y. (2009) Retaining Wall-Soil-Structure Interaction Effects Due to Seismic Excitation. *Earthquake Geotechnical Engineering Satellite Conference XVIIth International Conference on Soil Mechanics & Geotechnical Engineering*, Alexandria, Egypt.
- [15] Ali, A.F. and Mohammed, M.A. (2013) Soil-Structure Interaction of Retaining Walls under Earthquake Loads. *Journal of Engineering*, **19**.
<https://doi.org/10.31026/j.eng.2013.07.03>
- [16] Gupta, H., Gopalakrishnan, N., Agrawal, P. and Mukherjee, M. (2023) Seismic Behaviour of Dry Stack Stone Masonry—A Numerical Study. *Proceedings of 17th Symposium on Earthquake Engineering*, **2**, 695-703.
https://doi.org/10.1007/978-981-99-1604-7_52
- [17] Nougier, J.P. (1987) Methodes de Calcul Numérique. University of Montpellier.
- [18] Kumeso, N.H. (2014) Calculparasismique des pylônes dans la zone Est de la DRC. Ph.D. Thesis, Université de Kinshasa, Kinshasa.
- [19] Buhendwa, V.M. (2018) Information Management in the Monitoring of Nyamulagira

- and Nyiragongo Volcanoes in Eastern Democratic Republic of Congo. <https://hal.science/hal-01901969>
- [20] Gutierrez, E.S., Sahdia, K. and Crété, E. (2019) Detailed Shelter Response Sheet Democratic Republic of Congo (South-East): Local Constructive Cultures for Sustainable and Sustainable Habitats Resilient Habitats. CRAterre.
- [21] Choudhury, D. and Ahmad, S.M. (2007) Stability of Waterfront Retaining Wall Subjected to Pseudo-Static Earthquake Forces. *Ocean Engineering*, **34**, 1947-1954. <https://doi.org/10.1016/j.oceaneng.2007.03.005>
- [22] Ghosh, P. (2008) Seismic Active Earth Pressure Behind a Nonvertical Retaining Wall Using Pseudo-Dynamic Analysis. *Canadian Geotechnical Journal*, **45**, 117-123. <https://doi.org/10.1139/T07-071>
- [23] Tiwari, R. and Lam, N. (2022) Displacement-Based Seismic Evaluation of Base-Retained Retaining Walls. *Acta Geotechnica*, **17**, 3675-3694. <https://doi.org/10.1007/s11440-022-01467-y>
- [24] Nian, T.K., Liu, B., Han, J. and Huang, R.Q. (2014) Effect of Seismic Acceleration Directions on Dynamic Earth Pressures in Retaining Structures. *Geomechanics and Engineering*, **7**, 263-277. <https://doi.org/10.12989/gae.2014.7.3.263>
- [25] Li, S.H., Cai, X.G., Xu, H.L. and Jing, L.P. (2020) Dynamic Behaviour of Reinforced Soil Retaining Wall under Horizontal Seismic Loading. *IOP Conference Series Earth and Environmental Science*, **569**, Article ID: 012001. <https://doi.org/10.1088/1755-1315/569/1/012001>
- [26] Thill, M. and Cimanuka, A. (2019) La gouvernance de la sécurité à l'est du Congo. Décentralisation, réforme de la police et interventions dans la chefferie de Buhavu. Open Street Map, Rift Valley Institute.
- [27] Mavonga, T. (2009) Seismic Hazard Assessment and Volcanogenic Seismicity for the Democratic Republic of Congo and Surrounding Areas, Western Rift Valley of Africa. Ph. D. Thesis, University of Witwatersrand, Johannesburg.
- [28] NF EN 1998-1 (2005) Eurocode 8: Design and Dimensioning of Structures for Earthquake, Part 1: General Rules—Seismic Actions. CEN-AFNOR (Commission Association française de normalisation), Paris, 75-91.
- [29] Khan, M.M. and Javid, S.M. (2019) Seismic Behaviour of Rcc Multi Storey Building with Retaining Wall. *International Journal of Engineering Development and Research*, **7**, 92-103.
- [30] NF EN 1997-1 (2004) Eurocode 0: Bases de calcul des structures, AFNOR. CEN-AFNOR (European Commission for Standardization—French Association française de normalisation).
- [31] NF EN 1997-1 (2004) Eurocode 7: Geotechnical Design, Part 1: General Rules. CENAFNOR (Commission Européenne de Normalisation—Association Française de Normalisation), Paris.
- [32] NF EN 1997-1 (2004) Eurocode 2: Design of Concrete Structures, AFNOR. CEN-AFNOR (European Commission for Standardization—French Association for Standardization).
- [33] NF EN 1997-1 (2004) Eurocode 6: Calculation of Masonry Structures—Part 2: Calculation, Choice of Materials and Implementation of Masonry AFNOR. CEN-AFNOR (Commission Européenne de Normalisation—Association française de normalisation).
- [34] Setra (1998) Retaining Structures, General Design Guide. Technical Studies Service for Roads and Highways, CTOA, Bagneux Cedex.

Appendix

Typical values for the mechanical properties of soils in the shear test.

Floors	soil permeability index (%)	Internal angle of friction ϕ_s (degrees)	Soil cohesion c (kPa)
Crushed rock		47 ± 7	0
Clean gravel	0	40 ± 5	0
Silty gravel	2 - 6	36 ± 4	≈ 0
Clay gravel	7 - 12	34 ± 4	≈ 0
Clean sand with large grain size	0	40 ± 4	0
Clean sand with uniform grain size	0	36 ± 6	0
Slightly to moderately silty sand	2 - 6	34 ± 3	≈ 0
Slightly to moderately clayey sand	6 - 12	32 ± 3	≈ 0
Clayey sand	9 - 15	27 ± 3	5 ± 5
Silt	2 - 6	33 ± 4	≈ 0
Clayey silt	4 - 10	30 ± 4	15 ± 10
Silty clay	12 - 18	27 ± 4	20 ± 10
		-20	20 ± 10
		-40	25 ± 10
Clays		-60	2
		>100	<8